



Eidgenössische Technische Hochschule Zürich  
Swiss Federal Institute of Technology Zurich

# Design, Build-up and Control of Electronic Equipment for the Hybrid Rydberg Experiment

Mario S. Könz

May 8, 2014

Supervisor:

Tobias Thiele

Technical Supervisor:

Hansjürg Schmutz

Principal Investigator:

Prof. Andreas Wallraff

## Abstract

In this thesis the following tasks were achieved: 1) a LabView driver for the digital delay generator SRS DG645 was programmed. This allowed the main LabView framework of the entire hybrid Rydberg experiment to control the digital delay generators. 2) High voltage control electronics were constructed for applying potentials to a multi channel plate (MCP). This allows to apply high voltage bias to the different plates of the MCP and to read out its electronic signal. Its thus possible to switch its gain from  $\sim 1600$  V to  $\sim 2000$  V in 60 ns for only being sensitive to one part of the signal in time. This reduces the later charge transfer due to metastable atoms which decreases the MCPs lifetime. 3) With the help of an integrating amplifier (IA), the temporal signal was integrated and amplified (gain 15). The behavior of the IA can be adjusted with a variable capacity and resistor. Finally, (4), a spectrum of singlet  $1s^1 2s^1 \ ^1S_0$  He was measured and its frequencies compared to the theory.

# Contents

<b>1</b>	<b>Introduction</b>	<b>1</b>
1.1	Hybrid Quantum System . . . . .	1
1.2	Rydberg Atoms . . . . .	1
1.3	Setup . . . . .	2
<b>2</b>	<b>Micro Channel Plate Detector</b>	<b>5</b>
<b>3</b>	<b>LabView Driver for the DG645</b>	<b>7</b>
3.1	Digital Delay Generator . . . . .	7
3.2	Implementation of the driver . . . . .	7
<b>4</b>	<b>High Voltage Support Electronics for the MCP</b>	<b>11</b>
4.1	Purpose . . . . .	11
4.2	In/Outputs . . . . .	11
4.3	Circuit Schematics . . . . .	14
4.4	Manufacturing . . . . .	16
4.5	Initial Measurements . . . . .	16
4.6	Measurement with optimization . . . . .	16
4.7	Final Measurements . . . . .	18
<b>5</b>	<b>Integrating Amplifier</b>	<b>20</b>
5.1	Purpose . . . . .	20
5.2	Circuit Schematics . . . . .	20
5.3	Manufacturing . . . . .	22
<b>6</b>	<b>Spectrum of Helium</b>	<b>24</b>
<b>7</b>	<b>Summary</b>	<b>26</b>
<b>A</b>	<b>Appendix</b>	<b>27</b>
A.1	LabView Code . . . . .	27
A.2	SE Measurements . . . . .	29
A.3	Startup Procedure . . . . .	34
A.4	PCB Manufacture with the Etching Method . . . . .	36
	<b>List of Figures</b>	<b>38</b>
	<b>References</b>	<b>39</b>

# 1 Introduction

This thesis was done in a group in the Quantum Device Lab of Professor Andreas Wallraff. My main supervisor, Tobias Thiele, studies the behavior of hybrid quantum systems. The experiment aims at coupling Rydberg atoms with microwave photons in a transmission line. The following sections explain the different components needed for this to work.

## 1.1 Hybrid Quantum System

Today much effort flows into the research of a potential physical implementation of a quantum computer. Such a machine would be based on a qubit instead of a classical bit that computers nowadays use. There are many tasks that are expected to run more efficient (i.e. in a different complexity class) with quantum algorithms on a quantum computer than on its classical counterpart, which makes the quantum computer very interesting. In the classical computer storage and processing are done by transistors that implement a bit. The challenge for developing a quantum computer is finding the quantum counterpart to the transistor, a stable physical implementation of the qubit. Today, science still faces two problems: First one would need to have many qubits (for comparison: there are 1.4 billion transistors on a Intel Haswell architecture / one would need far less qubits due to the exponential growth of states) on a small space while still being able to address and manipulate each one direct or indirect. The second challenge is to store a qubit over a long time. The problem lies in the nature of excited quantum states, since they decay to the ground state after a certain time (known as the decoherence time). This time depends on the coupling strength to the environment. But decreasing the coupling also prolongs the time needed to perform an operation, thus the number of operation on a given qubit is limited due to decoherence.

The hybrid quantum system addresses this problem by using two different physical implementation of the qubit with different coherence times. The main idea proposes to do the operation on a strongly coupled qubit (i.e. Transmon) and then transferring the information to a weakly coupled one (i.e. Rydberg atom) in order to store it. Figure 1 shows this idea. The Rydberg atoms could act as RAM for a quantum computer. For more details about the quantum hybrid system see [8] .

## 1.2 Rydberg Atoms

A Rydberg atom is an excited atom characterized by a high principle quantum number  $n$  ( $\geq 18$ ). In such a state one valence electron (or more) is far away from the core (core electrons and nucleus). For this electron (and sufficient large distance from the core) the core looks like a Hydrogen nucleus. Only for states with low angular momentum (as they have non-zero probability to be inside the core) one needs correction. This correction is called the quantum defect  $\delta_l$  and

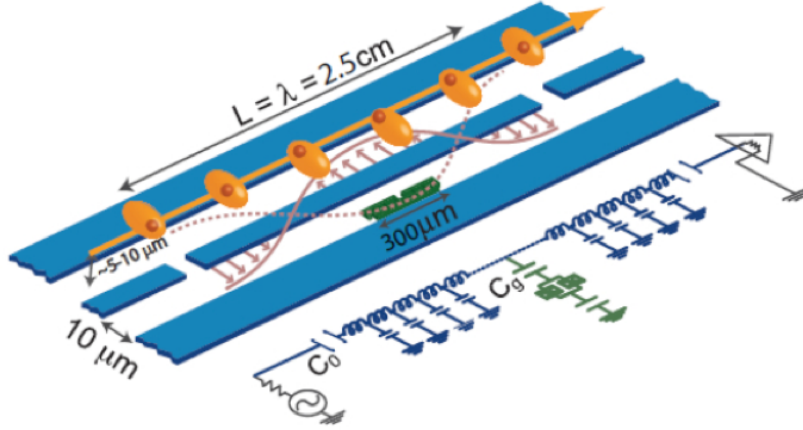


Figure 1: The Rydberg atoms (orange) fly above a coplanar transmission line (blue) that contains an artificial atom (Transmon / green). The superconducting charge qubit acts as the processor, while the Rydberg atoms act as memory to store quantum information for a longer period of time ( $\approx ms$ , see Section 1.2) since the coherence time is too short on the superconducting qubit ( $\approx \mu s$ ).

is small for large  $l$  and of order 1 for low  $l$ . The binding energy of the electron is given by:

$$E_n = -\frac{R_y}{(n - \delta_l)^2} \quad (1)$$

Because the electron and the core are separated by a large distance ( $\propto n^2$ ), the Rydberg atom is an excellent dipole ( $\sim 1500a_0e$  for  $n = 60$ ). The energy difference between neighboring states is proportional to  $n^{-3}$ . For  $n > 25$  the wavelength needed to drive a transition is in the range of  $\mu m - mm$ . Furthermore the lifetime (coherence time) scales with  $n^3$  for low  $l$  and with  $n^5$  for large  $l$  ( $\tau = 70 ms$  for  $n = 60, l = 59$ , see [3]). Rydberg atoms have a very long coherence time compared to other quantum systems and are therefore a promising candidate to store quantum information. More about Rydberg atoms can be found in [3] or [4].

### 1.3 Setup

A sketch of the experiment is shown in Figure 2. The pulsed valve (25 Hz) generates a supersonic Helium beam (length:  $190 \mu s / v_s = 1.7 \frac{km}{s}$ ). 2 mm after the valve an electric HV-pulse ( $20 \mu s / 250 V$ ) generates a He-plasma. Some ions recombine to a metastable state ( $1s^1 2s^{11} S_0$ ). The beam passes a skimmer in order to collimate before being hit by UV laser pulse<sup>1</sup> ( $313 nm / 10 ns$

<sup>1</sup>The UV laser is realized with a frequency doubled Nd:Yag pumped dye-laser.

/  $0.5 \frac{\text{mJ}}{\text{pp}}$ ) between electrode 1 and 2 that excites the metastable He-atoms to a  $np$  state ( $n \approx 34$ ). To minimize the negative effect of the blackbody radiation (for the coherence time) and enable the superconductivity of the artificial atom, the central part of the experiment is cooled down to 3 K. When the excited He-atoms pass over the coplanar transmission line they couple to the cavity and the information from the artificial atom (that also couples to the cavity) can be transported onto these excited He-atoms. Due to this process, the states of the He-atoms can change. Before leaving the 3 K stage, state-selective field ionization is applied to the excited He-atoms (between electrodes 3 and 4) using an electric field pulse (1.2 kV/10 ns). The resulting electrons/ions are accelerated towards the MCP (multi channel plate) and their spatial and temporal signal is detected (see Section 2). The temporal signal from the MCP is amplified and sent to an oscilloscope. The oscilloscope transforms the analog signal and sends a digital signal to a computer. The main LabView framework that runs on this computer further integrates a selected region of the incoming signal and stores the result in a datafile. Appendix A.3 shows the startup procedure for the experiment. It was accurate up to June 2012 and may be outdated now since the experiment moved into another lab.

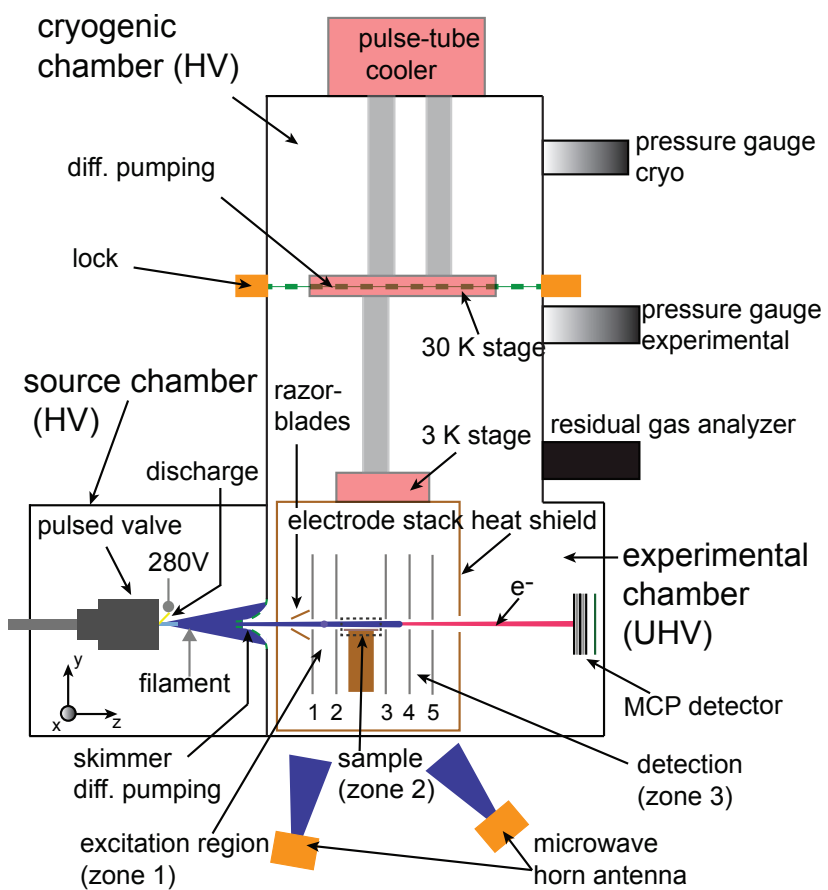


Figure 2: The setup of the experiment. Section 1.3 describes the process in detail.

## 2 Micro Channel Plate Detector

The micro channel plate (MCP) is a single particle detector, which is used to detect the Rydberg electrons. As in an electron multiplier the mechanism uses secondary emission of electrons to amplify the few incoming particles. The MCP consists of many channels that are tilted in one direction and after the middle in the other one (Figure 4, A). This ensures that incoming particle hit the walls of the channels. If charged, the particles are accelerated towards the MCP by a difference in the applied electric potential between the MCP and their place of origin. The incoming particle hits the wall of the channel (Figure 4, B) and causes secondary emission of electrons (Figure 4, C). This avalanche-effect continues until many electrons leave the MCP at D (Figure 4) and are accelerated towards a detector like a phosphor screen with a CCD for example, again by a potential difference. The key advantage over a normal photon multiplier lies in the MCP's ability to also provide a spatial signal<sup>2</sup>. Figure 3 shows a very similar setup of the MCP that is used in this setup. The MCP used in this experiment is an APD 2 40/12/10/8 I 60:1 EDR P47 manufactured by Photonis. This stands for: quality diameter 40 mm / Pitch center-to-center 12  $\mu\text{m}$  / pore diameter 10  $\mu\text{m}$  / bias angle 8 deg (angle in which the channels are tilted) / MCP Grade Image / Aspect ratio 60:1 (diameter to length) / rimmed / Extended Dynamic Range (increases detection limit<sup>3</sup> by factor 10). [6] will explain the detailed meaning of this product code further. The gain is of the order  $\sim 10^7$  for such a MCP and a voltage difference between front and back of  $\sim 2400$  V.

It is obvious that the gain depends strongly on the electric potential difference between the front and back of the MCP. Furthermore the MCP has a limited lifespan depending on the charge transferred (i.e. knocked out electrons). To prolong the lifespan one can increase a default potential if the interesting signal/particles (Rydberg electrons) hit the MCP. The uninteresting particles (metastable atoms / Rydberg atoms / ions / UV laser photons) are only amplified by the default potential. The electric potential difference between the front and back is lower in the default state but can be risen to increase the gain.

For all this to work, different support electronics is needed. Building this electronics and integrating the devices to the main control of the hybrid Rydberg experiment was the task of this work. The following sections describe the electronics needed for the MCP to work.

---

<sup>2</sup>together with an appropriated detector like a CCD.

<sup>3</sup>After one detection, a channel needs to recharge its lost electrons and is less sensitive to an event that follows during this recharge time.



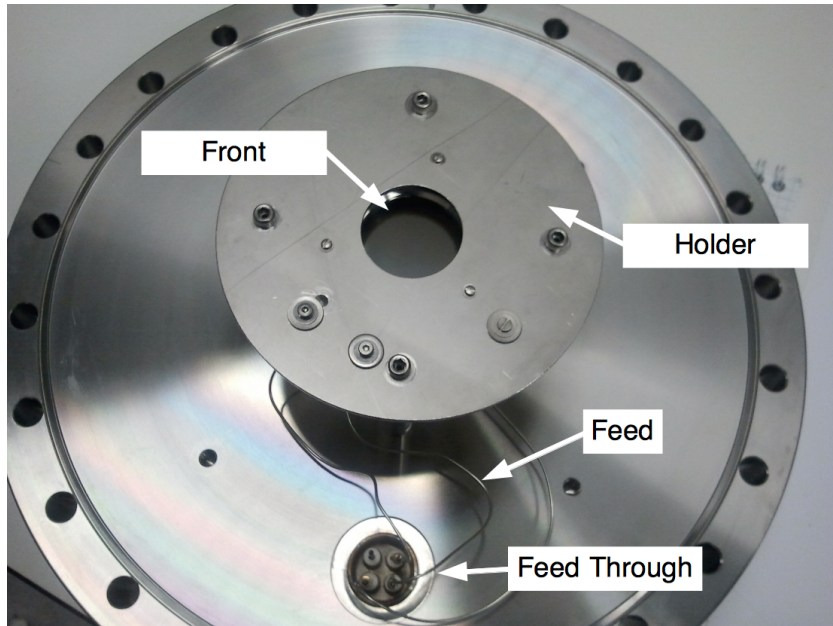


Figure 3: The MCP setup used in this experiment. The MCP is mounted onto the back of the holder. A feed through passes the feed (signal) out of the vacuum chamber.

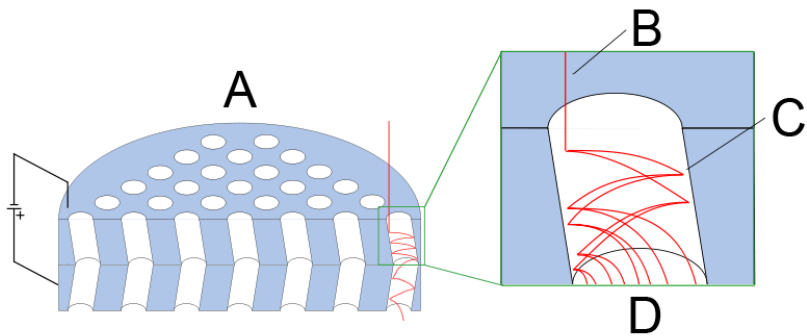


Figure 4: A: Tilted channels to ensure collision. B: An incoming particle hits the wall of the channel. C: Secondary emission of electrons. D: Electron cloud is accelerated towards the phosphor screen.

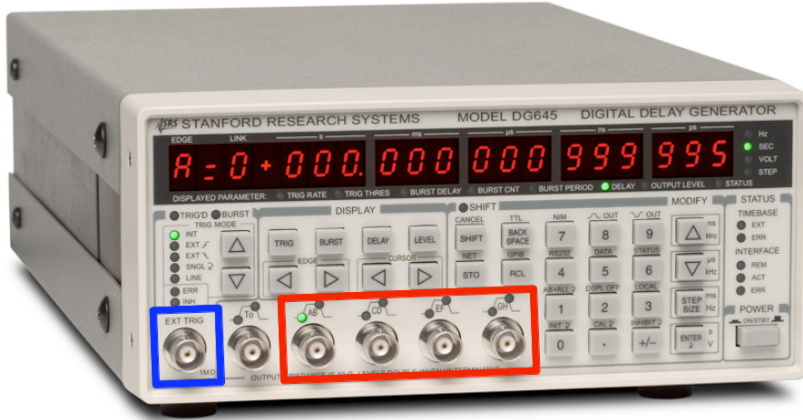


Figure 5: The SRS DG645 digital delay generator [7]. The blue box shows the external trigger input. The four programmable trigger lines are highlighted by the red box. The display and keypad allow to modify one value at a time.

### 3 LabView Driver for the DG645

#### 3.1 Digital Delay Generator

In the experiment, the different events and instruments need to be synchronized on a  $ns$ -timescale. For example the UV-laser pulse needs to be sent in the chamber when metastable He-atoms are in the center between electrode 1 and 2, electric potentials need to be applied to the MCP before the electrons hit the detector. Every device is triggered by an array of three digital delay generator (DDG). The first DDG is externally triggered by a main trigger (25 Hz). The two other DDG are externally triggered by the first one. We use the SRS DG645 [7] shown in Figure 5. One can set up to four trigger lines and specify the trigger start and end (0 s to 2000 s with 5 ps resolution), amplitude (0.5 V to 5.0 V) and offset ( $-2.0$  V to 2.0 V). The DG645 can be connected via Ethernet. For this a virtual COM-Port is generated in order to communicate via RS-232 with the DG645. For easy operation, a driver and GUI (graphical user interface) was build, using LabView. This allows the user (with the GUI) and the main control of the hybrid Rydberg experiment (with the driver) to check and change all trigger line values of the three DDG.

#### 3.2 Implementation of the driver

The task of the LabView driver is to enable software control over the DG645. The DG645 comes with a specified set of low-level commands that allow operating the device remotely. Figure 6 shows a few commands with description.

*SRE(?) <i>{i}</i>	Page 49	Service Request Enable
*STB?	Page 49	Status Byte
*TRG	Page 50	Trigger a delay
*TST?	Page 50	Self Test
*WAI	Page 50	Wait for Command Execution

---

### Status and Display Commands

DISP(?) <i>{i,c}</i>	Page 50	Display
INSE(?) <i>{i}</i>	Page 51	Instrument Status Enable
INSR?	Page 51	Instrument Status Register
LERR?	Page 51	Last Error
SHDP? <i>{i}</i>	Page 51	Show Display
TIMB?	Page 51	Timebase

---

### Trigger Commands

ADV <sub>T</sub> (?) <i>{i}</i>	Page 52	Advanced Triggering Enable
HOLD? <i>{t}</i>	Page 52	Holdoff
INH <sub>B</sub> (?) <i>{i}</i>	Page 52	Inhibit
PHAS(?) <i>i{,j}</i>	Page 52	Prescale Phase Factor
PRES(?) <i>i{,j}</i>	Page 52	Prescale Factor

Figure 6: Example of some commands [7, p 46] that had to be translated by the driver. The syntax in the left column is the actual command that is sent via RS-232 to the device.

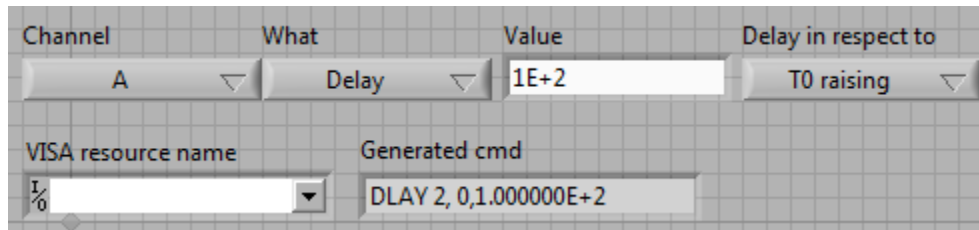


Figure 7: This part of the GUI allows to choose the channel (A-H), variable (delay, step, offset) and value and shows the command that is sent to the DG645. The VISA resource name would be one DG645. Figure 19 in Appendix A.1 shows the corresponding part of the driver.

The driver connects these commands with a more practical LabView interface for user, called VI (virtual instrument). Other LabView scripts can use this VI as part of their process. Based on the driver, a GUI further simplifies the remote control of the DG645. To better understand the driver and GUI, we consider the following example: The user wants to change some value of one trigger line of one DG645. The GUI shown in Figure 7 can be used to conveniently select the channel (A / each trigger line consists of two channels, begin and end), the variable (delay), its value ( $1E+2$ ) and the reference point for the delay (T0 rising<sup>4</sup> / only needed for the delay variable). With the VISA resource name one can choose which DG645 should be addressed. Figure 19 in Appendix A.1 shows the part of the driver, that translates the informations given by the user to a valid DG645 command. This command (see bottom center of Figure 7) is sent via a RS-232 connection to the DG645 and changes the delay of channel A to  $1E+2$  with respect to T0 rising.

Figure 18 in Appendix A.1 shows the part of the driver that reads all values of the four trigger lines and stores them into a matrix. Once written, this block may be reused by other LabView scripts. The GUI to the full driver shown in Figure 8 can support up to three DG645 and read and write all trigger line. With this driver one can trigger the electric potential changes for the MCP. But since the DG645 only supports small voltages (5 V) another device is needed to support large voltage changes (400 V). This device is the high voltage switch described in the next section.

---

<sup>4</sup>the leading edge of T0 is the zero time reference, see [7]

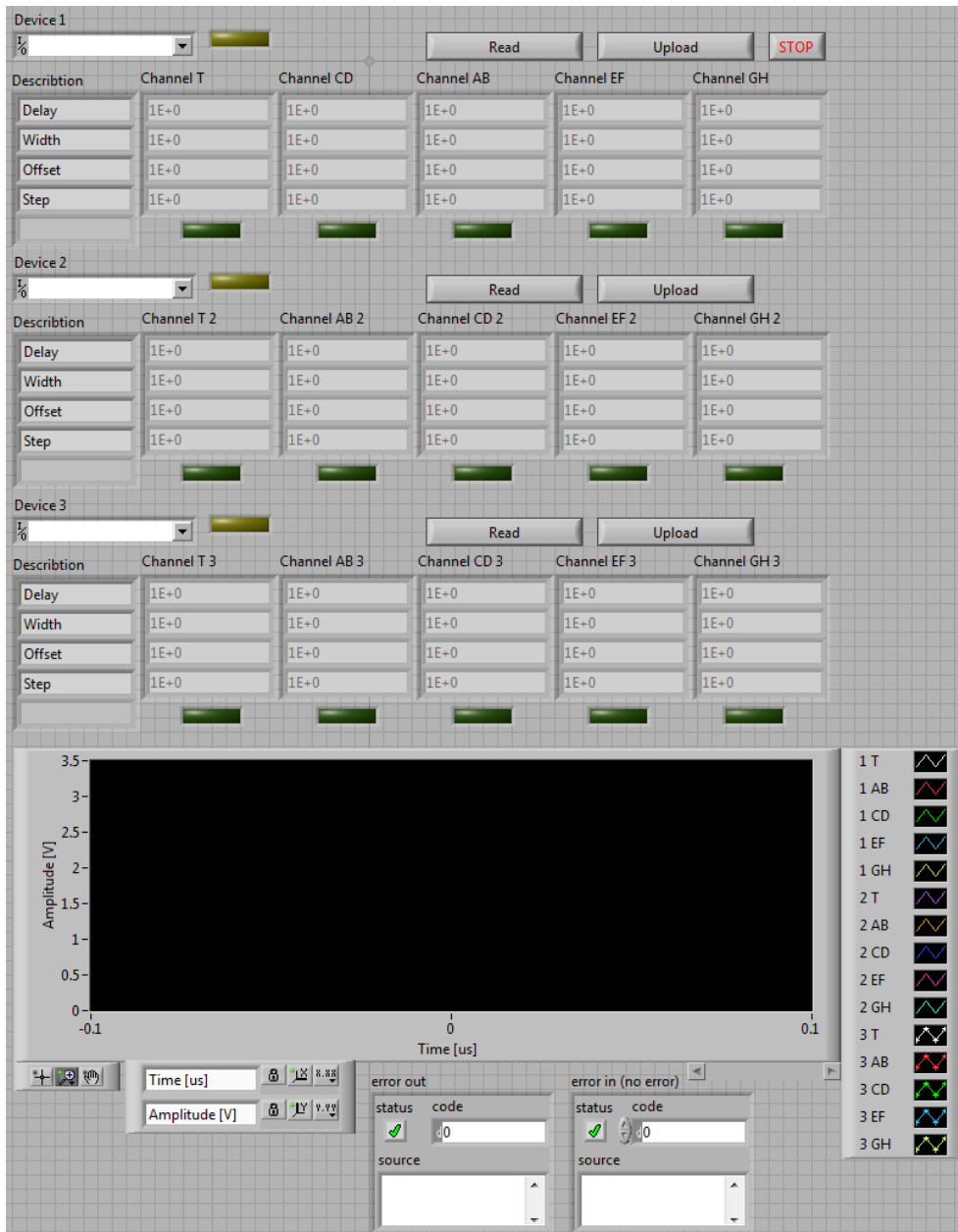


Figure 8: The GUI of the full driver is able to control up to three DG645. Every trigger line variable belonging to these DG645 can be read and written. The plot at the bottom of the figure shows the trigger pulses graphically when devices are attached.

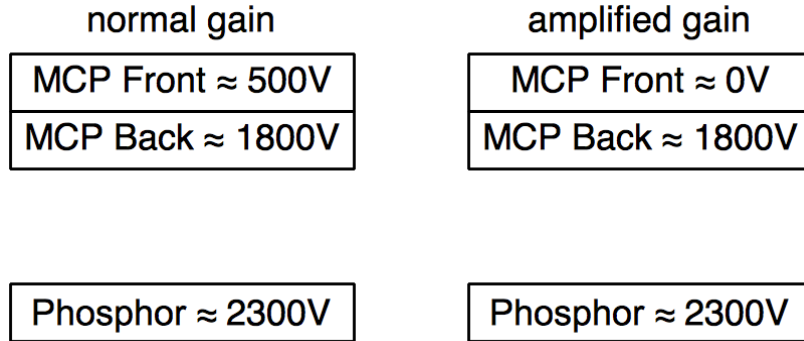


Figure 9: The HV-Switch of the SE reduces the front potential by  $\approx 500$  V to detect the Rydberg electrons with an amplified gain. The normal/reduced gain prolongs the lifetime of the MCP during the detection of uninteresting particles.

## 4 High Voltage Support Electronics for the MCP

### 4.1 Purpose

The support electronics (SE) for the MCP has the following components:

- an adapter that connects the high voltage sources to the corresponding parts of the MCP. Where necessary we introduced filters to remove noise from the sources as well as back-up capacities to provide charge when needed. When a particle is detected, MCP front and back lose electrons that need to be replenished. The back-up capacities speed up this process. A red box named core in Figure 10 shows this part.
- a high voltage switch (HV-Switch) capable of switching up to 500 V in a fast manner (60 ns). This allows to amplify the gain when needed (see Section 2). Figure 9 shows the electric potentials on the different MCP part in the electron detection mode. Figure 10 shows this part in a red box named HV-Switch.
- a channel that allows to read the temporal signal of the MCP. If a particle hits the detector, a large amount of electrons/current (proportional to the gain) flows from the MCP front plate to the back plate. This current can be detected to get the temporal signal (see Section 4.3). It can be found in Figure 10 labeled as H.

The three terms Core, HV-Switch and optimization used in the next section refer to the parts framed by red boxes in Figure 10.

### 4.2 In/Outputs

This section lists the in- and outputs of the SE. Figure 10 shows the final circuit schematics. The different elements of the circuit are explained in detail in

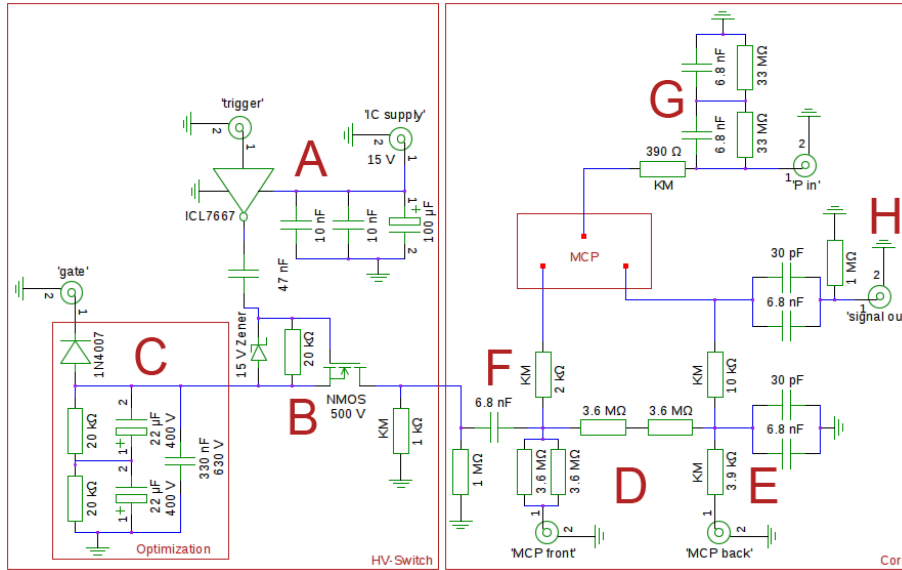


Figure 10: The circuit schematics of the SE. The in- and outputs (two concentric green circles / square red dots) are listed in Section 4.2 while the detailed explanation of part A-H can be found in Section 4.3.

Section 4.3.

The SE has these inputs:

SHV (safe high voltage connector)

- MCP front  
'FRONT IN' is set to GND for the measurement of Rydberg electrons
- MCP back  
'BACK IN' supplies the second plate of the MCP. In this setup it is around 1800 V
- Phosphor  
'P IN' is used to bring the phosphor-plate to the right potential, in order to get the spatial signal. It is set mostly to 2200 V for just the temporal signal or to 5000 V for the spatial signal. The higher voltage accelerates the electrons towards the phosphor plate where they produce the spatial signal.

BNC (Bayonet Neill–Concelman connector)

- Gate input  
'GATE' is always negative (so when the term "-" or added is used, keep in

mind, that 'GATE' is negative). It reduces the electric potential of 'FRONT OUT' if 'TRIGGER' is LOW. This leads to a bigger difference between 'FRONT OUT' and 'BACK OUT'. This helps to only amplify the interesting signals and increase the lifetime of the MCP.

- Signal out  
'SIGNAL OUT' provides the temporal signal.
- Trigger input  
'TRIGGER' controls the influence of 'GATE' on 'FRONT OUT'. If LOW, 'GATE' will be added to 'FRONT OUT'.
- 10-15V  
'IC SUPPLY' is needed for the IC in the setup.

The switch exposes three potentials:

- MCP front  
'FRONT OUT' goes to the front plate of the MCP. If 'TRIGGER' is HIGH (no additional 'GATE' potential), a voltage divider keeps the potential at  $\approx 0.2$  of 'BACK IN' potential. If 'TRIGGER' is LOW the potential is changed by 'GATE' i.e, 'BACK IN' = 2000 V, then 'FRONT OUT' = 400 V with 'TRIGGER' = HIGH and 'FRONT OUT' = 400 V + 'GATE' with 'TRIGGER' = LOW.
- MCP back  
'BACK OUT' is the connection that connects to the back plate of the MCP, and equal to 'BACK IN'.
- Phosphor  
'P OUT' is used to charge the phosphor-plate and is direct proportional to 'P IN'.

Figure 11 shows the location of the in- and outputs on the device and Figure 10 on the circuit schematics.

### Notation

Some useful notation, partly already used:

Name	Meaning
GND	ground potential
LOW	equal to GND
HIGH	potential of 5 V in respect to GND
$V_{fi}$	potential of 'FRONT IN' in respect to GND
$V_{bi}$	potential of 'BACK IN' in respect to GND
$V_{fo}$	potential of 'FRONT OUT' in respect to GND
$V_{bo}$	potential of 'BACK OUT' in respect to GND
$V_{diff}$	$V_{bo} - V_{fo}$
$V_g$	potential of 'GATE' in respect to GND



### 4.3 Circuit Schematics

As outlined in Section 4.1 the SE allows to measure a temporal signal of the incoming Rydberg electrons. Since this Rydberg electrons are amplified in the MCP via secondary emission of electrons and are then accelerated towards the back plate, a current flows between 'FRONT OUT' and 'BACK OUT'. With the 'SIGNAL OUT' one can observe this current and calculate the impact time of the Rydberg electron. The spatial signal can be registered with a camera at the back of the phosphor plate. Many back-up capacitors store electrons in order to have a high current if the voltage changes. After the optimization, only negative 'GATE' potentials work due to the polar capacitors. The main focus was a maximal slew rate for the HV-Switch and error free transmission of high frequencies throughout the SE. Figure 10 shows the complete circuit of the SE and the following sections explain the parts A through H in detail.

#### Part A: MOSFET Driver

The 'TRIGGER' signal that is sent by the SRS DG645 ( $\approx 5\text{ V}$ ) isn't powerful enough to switch the NMOS transistor located at B. Therefore the MOSFET Driver ICL7667 [5] amplifies the 'TRIGGER' signal to the level needed to switch the transistor. It runs on a 15 V DC-supply that is supported by three back-up capacities. Without the back-up capacities the slew rate in the final 'FRONT OUT' potential would be much smaller. The 10 nF ceramic capacities react fast to changing potentials due to a low internal resistance. The larger 100  $\mu\text{F}$  electrolytic capacitor recharges the ceramic capacities if needed. Note that the driver inverts the incoming pulse. One has to change the 'TRIGGER' line from HIGH to LOW in order to trigger the transistor.

#### Part B: NMOS Gate

The NMOS transistor FQP5N60C [2] is used to add the 'GATE' potential to the 'MCP FRONT'. The potential difference between part A and part B/C require DC-decoupling, which is realized with a 47 nF ceramic capacitor. We do not need an optocoupler since we are only interested in sending short pulses and all high frequencies can pass the capacitor. The potential in part B/C is negative so that a +15 V pulse opens the NMOS transistor. As a safety measure, a Zener Diode protects the transistor from a too large source/drain potentials ( $> 15\text{ V}$ ). Since there are no inductive elements connected to this part, it is only necessary if the MOSFET driver is supplied with more than 15 V.

#### Part C: Optimization

To ensure a fast ( $\sim 60\text{ ns}$ ) potential switch at the 'FRONT OUT' these back-up capacitors store the energy needed for a later release. The ceramic capacitor provides the energy (discharges) very fast due to the low internal resistance. The electrolytic back-up capacitors recharge the ceramic capacitor if needed. They charge/discharge slower because of a higher internal resistance but have

a larger capacity. The resistors protect the electrolytic capacitors since they are rated for 400 V.

#### Part D: MCP Potentials

The four 3.6 M $\Omega$  resistors form a voltage divider. If 'FRONT IN' is set to GND the potential of 'FRONT OUT' should be 0.2 of 'BACK IN'<sup>5</sup>. Figure 12 shows the measurement plot  $V_{bi}$  vs.  $V_{diff}$ . The measurement showed a ratio of  $\frac{V_{diff}}{V_{bi}} = 0.8$  and confirmed the theoretical ratio of  $\frac{V_{fo}}{V_{bi}} = 0.2$ .

#### Part E: Low-Pass Filter

A low pass filter removes the noise spectrum of the clocked voltage supply and voltage peaks from the signal line. The high frequencies leave the main line via the two capacities. The reason for two different capacities is the hidden inductance that every capacitor has, that blocks too high frequencies. With two capacities in parallel a broader high-frequency-band can pass the system. KM stands for carbon composition resistors. These resistors have a very small inductance compared to metal film resistors and interact less with high frequencies and are thus used throughout the signal line.

#### Part F: Gate Coupling

A 6.8 nF capacitor DC-deouples the HV-Switch from the Core. The carbon composition resistors (KM) have the advantage to handle high currents for a brief moment without taking damage, which is important for a fast change in the MCP potential. There is a small capacity between 'FRONT OUT' and 'BACK OUT' formed by the plates of the MCP. When changing 'FRONT OUT' by 'GATE' the additional energy for this capacitor has to flow as fast as possible through the resistors and carbon composition resistor are thus the best choice.

#### Part G: Phosphor Potential

Similar to the current mentioned in the beginning of 4.3 a current flows between 'BACK OUT' and 'P OUT' if electrons hit the Phosphor plate while the spatial signal is recorded. Two capacities are installed to store the incoming electrons and speed up the recharge process.

#### Part H: Signal Output

This capacitor setting looks identical to part E but serves a different purpose. High frequency signal pass these capacities towards 'SIGNAL OUT'. The current mentioned in part G flows through 'SIGNAL OUT' not 'MCP BACK'. It is advantageous to keep a pre-amplifier close to the SE in order to make the circuit as short as possible, because of the pulses / high frequencies involved. With the

---

<sup>5</sup>Calculation:  $\frac{R_{front}}{R_{tot}} = \frac{R_{front}}{R_{front} + R_{back}} = \frac{(\frac{1}{3.6\text{M}\Omega} + \frac{1}{3.6\text{M}\Omega})^{-1}}{(\frac{1}{3.6\text{M}\Omega} + \frac{1}{3.6\text{M}\Omega})^{-1} + 2 * 3.6\text{M}\Omega} = 0.2$

integrating amplifier (see Section 5) one can enhance the signal before sending it to an oscilloscope for time-based detection.

#### 4.4 Manufacturing

The Core was built first, then the HV-switch and last the optimization (see Figure 10, Part C). Because of the high voltages (3000 V) involved in this circuit, larger components were needed to meet the requirements (a PCB (printed circuit board) solution was not sensible). All parts were soldered in place using the input connectors as structural base (see Figure 11). The distance between certain wires had to be large enough to eliminate the risk of a bypass through air. Multiple holes for all connectors as well as for the screws that mount the device to the experiment were drilled. The three output potential that need to connect with the MCP have matched connectors (see green arrows in Figure 11).

#### 4.5 Initial Measurements

After constructing the core of the SE (see Figure 10), we needed the HV-Switch in proximity to it. Since the space allowed for a placement of the HV-Switch near the core it was installed in the same box (see Figure 11). The HV-Switch converts a logical pulse ( $\sim 5$  V) to a pulse with amplitude 'GATE'. To check the HV-Switch's functionality  $V_{fo}$  was measured at different 'GATE' potentials, different trigger-length and different 'IC SUPPLY' voltages. Figure 20 shows the results for different 'GATE' potentials. The voltage oscillations at the end of the rising edge are unfavorable. The amplitude of the voltage shows the expected values. In this measurements the trigger-length was set to  $20 \mu\text{s}$  and 'IC SUPPLY' to 15 V. Figure 21 shows the results for different trigger-length. A deviation from the expected voltage can be observed, if the trigger-length is set higher than  $20 \mu\text{s}$ . The yellow  $30 \mu\text{s}$  graph shows a dip in the plateau (horizontal part at  $\approx 50$  V), which increases with trigger-length. In this measurements 'GATE' was set to  $-350$  V and 'IC SUPPLY' to 15 V. The results for different 'IC SUPPLY' voltages is shown in Figure 22. It's possible to have a shorter plateau (horizontal part at  $\approx 50$  V) with decreasing 'IC SUPPLY', but there is a minimal limit ( $\approx 10$  V) after which the decay behaves irregular (see green 8 V graph). In this measurements 'GATE' was set to  $-350$  V and the trigger-length to  $7 \mu\text{s}$ .

Since the first measurement were not showing the desired properties we added a optimization in order to improve the HV-Switch. The main issues were the voltage oscillations on the rising edge and the strong dependence of the 'IC SUPPLY'. After the operating voltage for 'IC SUPPLY' is reached, a further increase mustn't have any influence.

#### 4.6 Measurement with optimization

After the installation of the optimization (see Figure 10) we performed a second measurement. The influence of this part is explained on Section 4.3 Part C.



Figure 11: The in- and outputs of the SE on the device. This pictures show the SE without the part Optimization (see Figure 10).

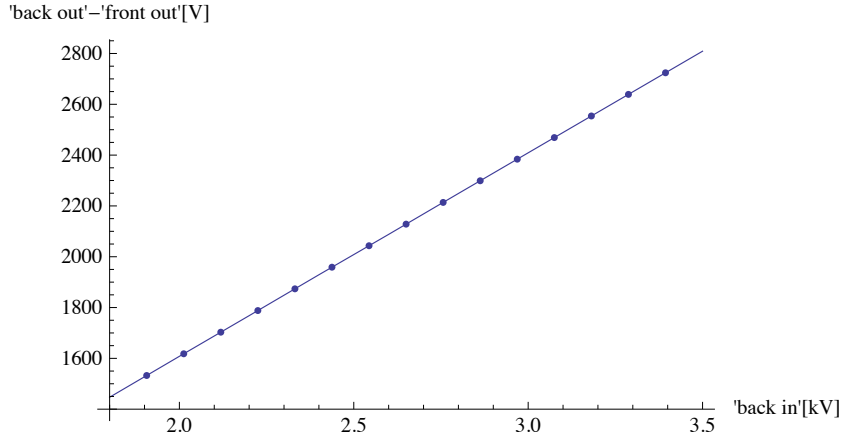


Figure 12:  $V_{diff}$  vs.  $V_{bi}$ . This linear behavior is expected due to the voltage divider between 'BACK IN' and 'FRONT OUT'.

Expected were smaller voltage oscillations on the rising edge and a steeper rising edge. The behavior of the HV-Switch was measured again at different 'GATE' potentials, trigger-length and 'IC SUPPLY' voltages. Figure 23 shows the results for different 'GATE' potentials. The voltage oscillations were reduced to an acceptable level, but an unexpected and undesired stretch of the timescale by a factor of  $\approx 10$  was observed. In this measurements the trigger-length was set to  $20 \mu s$  and 'IC SUPPLY' to 15 V. The results for different trigger-length are shown in Figure 24. The dip phenomenon (see Figure 21) at large trigger-length disappeared. But the trigger-length does not correspond to the length of the plateau (horizontal part at  $\approx 50$  V). The timescale is stretched compared to the first measurements. In this measurements 'GATE' was set to  $-350$  V and 'IC SUPPLY' to 15 V. Figure 25 shows the results for different 'IC SUPPLY' voltages. Note again the stretched timescale compared to the first measurement. In this measurements 'GATE' was set to  $-350$  V and the trigger-length to  $7 \mu s$ .

After solving the voltage oscillation problem, the large influence of the 'IC SUPPLY' onto the trigger-length remained. We tried a polarization change in the 'TRIGGER' input. This seemed sensible, since the gate of the NMOS transistor (see Figure 10) needs to be at a higher voltage as the source in order to open.

## 4.7 Final Measurements

After the change of the 'TRIGGER' polarization, we measured the behavior of the HV-Switch once more at different 'GATE' potentials, different trigger-length and different 'IC SUPPLY' voltages. Figure 13 shows the results for different 'GATE' potentials. The graphs show all desired properties like steep edges, correct voltages and durations. In this measurements the trigger-length was set to  $20 \mu s$  and 'IC SUPPLY' to 15 V. Figure 26 shows the results for different trigger-length. The change of the 'TRIGGER' polarization solved the problem of

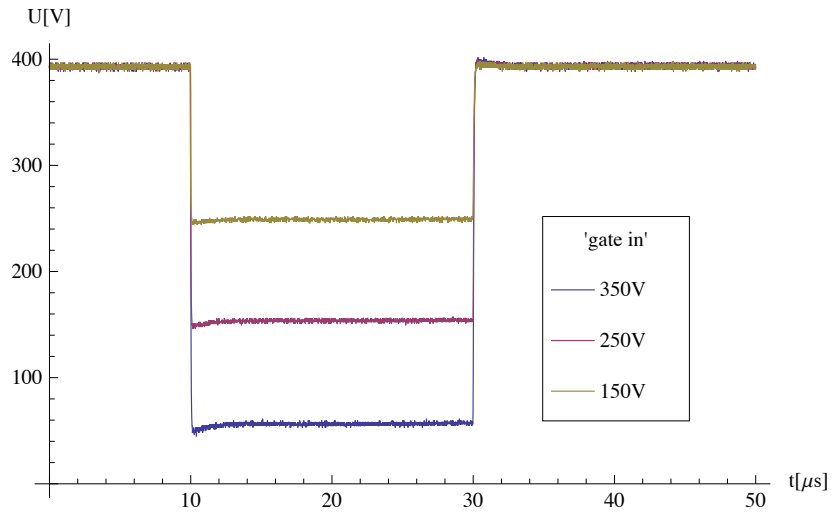


Figure 13:  $V_{fo}$  vs. time, with changing 'GATE' values after the polarization of 'TRIGGER'.

the timescale compared to Figure 24. In this measurements 'GATE' was set to  $-350\text{ V}$  and the 'IC SUPPLY' to  $15\text{ V}$ . Figure 27 shows the results for different 'IC SUPPLY' voltages. No dependence on the 'IC SUPPLY' in the range from  $8\text{ V}$  to  $15\text{ V}$  could be observed. This is expected since the MOSFET Driver is rated to work in this voltage section. In this measurements 'GATE' was set to  $-350\text{ V}$  and the trigger-length to  $7\text{ }\mu\text{s}$ .

These measurements confirmed, that the HV-Switch worked in the desired way.

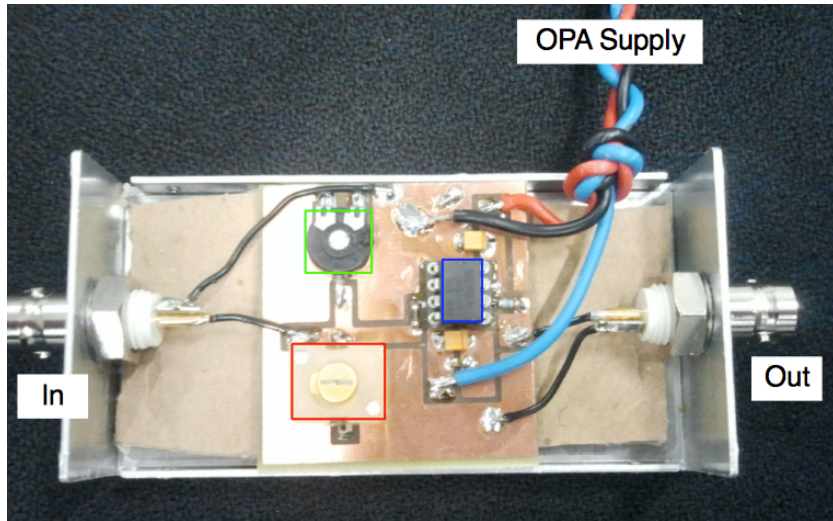


Figure 14: The signal of interest enters from the left (In) and is integrated with the OPA (blue box). The behavior of the integrator is determined by the variable resistor (green box) and capacity (red box). The integrated signal leaves on the right side (Out). Figure 15 shows the circuit schematics of the IA.

## 5 Integrating Amplifier

### 5.1 Purpose

As already mentioned in Section 4.3 short current pulse can be observed when the electron flow from the front to the back plate. This pulse needs to be amplified before being sent to an oscilloscope due to the low signal strength and high frequencies. The integrating amplifier (IA) shown in Figure 14 integrates the pulse and amplifies it with an operational amplifier (OPA). The integration time (explained in Part D: Integrator) as well as the capacity of the integrator circuit can be changed to optimize the signal gain.

### 5.2 Circuit Schematics

Figure 15 shows the circuit of the IA. Central piece is the OPA with the feedback loop. Part A to E explain the different components in detail.

#### Part A: Negative Feedback OPA

The main part of the IA is the OPA. We use the OPA637 [1] in conjunction with a negative feedback loop to limit the gain<sup>6</sup> to  $v = -\frac{1.5\text{ k}\Omega}{100\Omega} = -15$ . The negative

<sup>6</sup>This result assumes that the OPA can be treated as an ideal OPA and that it is not saturated.

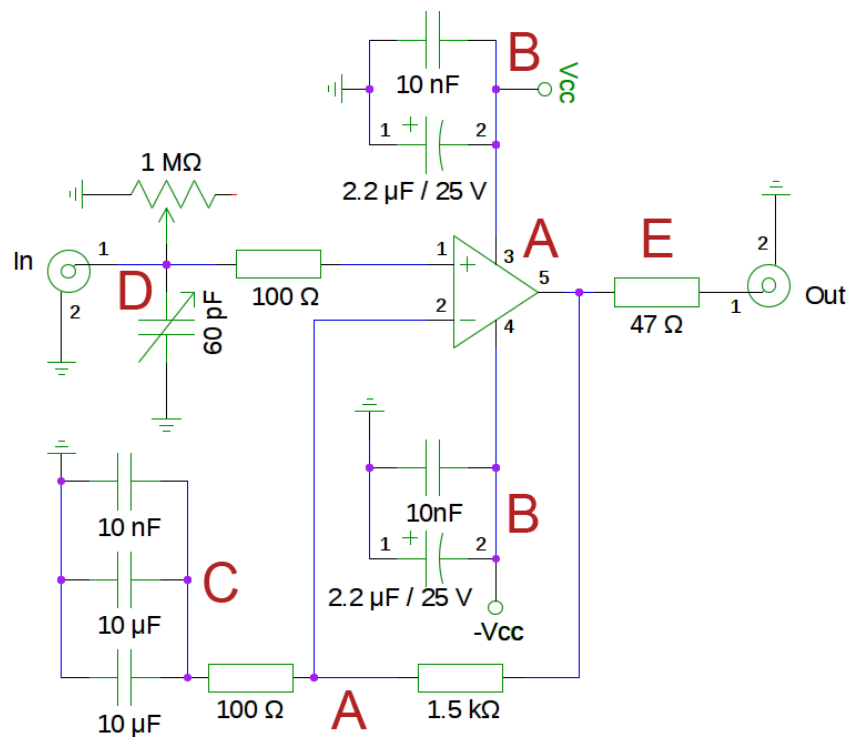


Figure 15: The circuit schematic for the IA. The OPA is the central part of this device. Due to the negative feedback loop (bottom A) the gain is equal 15.



sign just means that the polarization will change after the amplification.

### **Part B: Power Storage**

As in part A, E and G of the SE (see Figure 10) the back-up capacitors make sure that power is available when needed in order to amplify the signal properly. Again the ceramic capacitor reacts fast due to low internal resistance and the larger electrolytic capacity recharges the ceramic one if needed.

### **Part C: DC Gain Changer**

These three ceramic capacitors limit the gain for DC and very high frequencies ( $>100$  MHz) to one, because the capacitors behave like an open circuit for this cases (DC cannot pass a capacity / the internal hidden inductance of the capacities prevent very high frequencies from passing) and the negative feedback loop transforms into a buffer amplifier.

### **Part D: Integrator**

The signal to be amplified is a short pulse. To increase the signal, the whole pulse will be integrated in a 60 pF capacity. The capacity discharges via a 1 M $\Omega$  resistor. The discharge is chosen slower than the signal in order not to falsify it. The integration time is  $\tau = RC = 60 \mu\text{s}$ , short enough to reset the capacity in between signals and long enough to allow for correct integration. The integration time can be changed by changing the variable resistor and/or the variable capacity.

### **Part E: Impedance Matching**

One has to match the impedance of the output in order to prevent reflections due to the high frequencies involved. Reflections could damage the OPA or falsify the signal.

## **5.3 Manufacturing**

For this application the voltages were much smaller then for the SE and a PCB solution was possible. The double sided PCB was produced with the etching-process described in Appendix A.4 using Figure 16 as a template. All components were soldered in place by hand using a stereomicroscope (Laica MZ8) and a thin top solder head. The entrances for the in and output BNC connector, the hole for the OPA supply and the holes to access the variable resistor/capacity were drilled into the aluminum case.

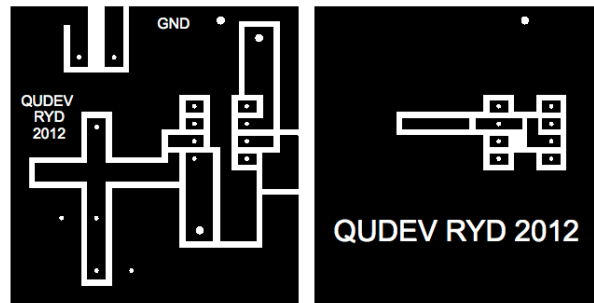


Figure 16: The PCB is 42 mm \* 43 mm in dimension. The white parts in this picture show where the copper is etched away. The exact procedure can be found in Appendix A.4. The top layer is shown left and the mirrored bottom layer right.

## 6 Spectrum of Helium

After building the SE and IA for the MCP, installing the MCP in the experiment and having integrated the DG645 driver into the main control of the hybrid Rydberg experiment measurements using the MCP were possible. We recorded the spectrum of singlet  $1s^1 2s^1 \ ^1S_0$  Helium. In this measurement the UV-laser swept from 624.300 nm to 629.000 nm in steps of 0.002 nm. Whenever an electron transition is energetically possible (i.e.  $2s \rightarrow np$ ) a Rydberg state is created. These states are ionized by pulsed field ionization for states  $n \geq 23$  and the Rydberg electrons detected by the MCP. Figure 17 shows the results. They agree with the theory of Rydberg atoms (see Section 1.2 and [3]). The quantum defect for these transitions is  $\delta_p = -0.01213$ . Figure 17 serves as a map to look up the laser frequency and wavelength that excites a certain state. The measured data is stored in *nm* of the laser frequency and integrated MCP signal. To obtain the energy we use:

$$E = \frac{hc}{\lambda}$$

The energy difference is given by:

$$\Delta E = E_\infty - E_n = h\nu = -h \frac{R_{He}}{(n - \delta_p)^2}$$

$R_{He}$  is the Rydberg constant for Helium, since the Helium has a different mass than Hydrogen. The value  $E_\infty$  is fitted using the  $n = 23$  measurement point.

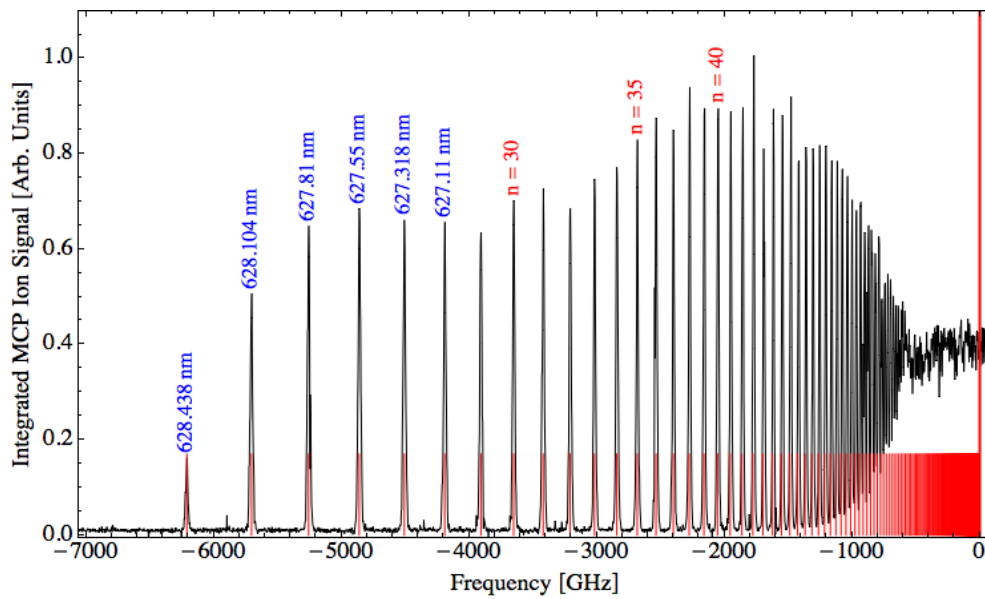


Figure 17: The black graph displays the detected Rydberg electrons at the MCP and shows indirect the absorption intensity. The red lines display the calculated values for singlet  $1s^1 2s^1 \ ^1S_0$  Helium. The tunable UV-laser swept from the  $n = 23$  to the ionization limit. The theoretical model and the measured data agree.

## 7 Summary

Four goals were achieved during this work:

1. SRS DG645 LabView driver: The driver works and is used by the main control of the hybrid Rydberg experiment.
2. High Voltage Support Electronics for the MCP: The SE prolongs lifetime of the MCP and provides all potentials necessary. Furthermore it also enables access to the temporal signal from the detected particles. This signal can be amplified and detected later. The main problem during the development was the usage of the wrong polarization on the 'TRIGGER'. The SE developed in this work is still in use with slight modifications.
3. Integrating Amplifier: This device amplifies the temporal signal from the SE. The current experiment uses a updated version of this device. The signal from 'SIGNAL OUT' has to be amplified in close proximity, since the pulse disperses while traveling long distances in cables and is even harder to detect then.
4. Spectrum of Helium: The spectrum of singlet  $1s^1 2s^1 \ ^1S_0$  Helium was measured and compared to the theory. The results agree with the theory and help to find the right UV-laser frequency for a certain transition. An A3-poster version of Figure 17 with more information was created in order to have such a map of the transitions.

This work was instructional, interesting and gave me an insight to experimental physics. I want to thank my supervisor Tobias Thiele for his advice and support, as well as Prof. Andreas Wallraff for taking me in for this work. Furthermore my thanks goes to Hansjürg Schmutz who helped me with all electronic challenges and components I was faced during this work. It was a valuable experience.

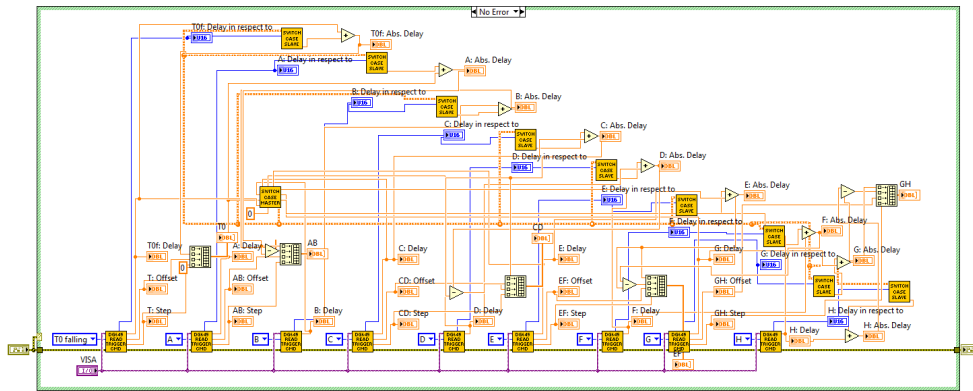


Figure 18: One part of the driver

## A Appendix

### A.1 LabView Code

Figure 18 shows the part of the driver that reads all variables of every trigger line of a given DG645 and returns its content as a matrix. Figure 19 shows the part of the driver needed to change a variable on a channel. The top left fields “Channel”, “Value” and “Delay in respect to” are the input values. The three center boxes process the input values and correspond to the different commands available. The top right field “What” determines which command is used. The bottom yellow line opens (yellow box with letter O) a VISA (Virtual Instrument Software Architecture) resource (a DG645), writes the translated command to it (yellow box with letter W) and closes the resource again (yellow box with letter C). Figure 7 shows the corresponding part of the GUI. The use of the parts shown in Figure 18 and 19 can be found in Section 3.2.

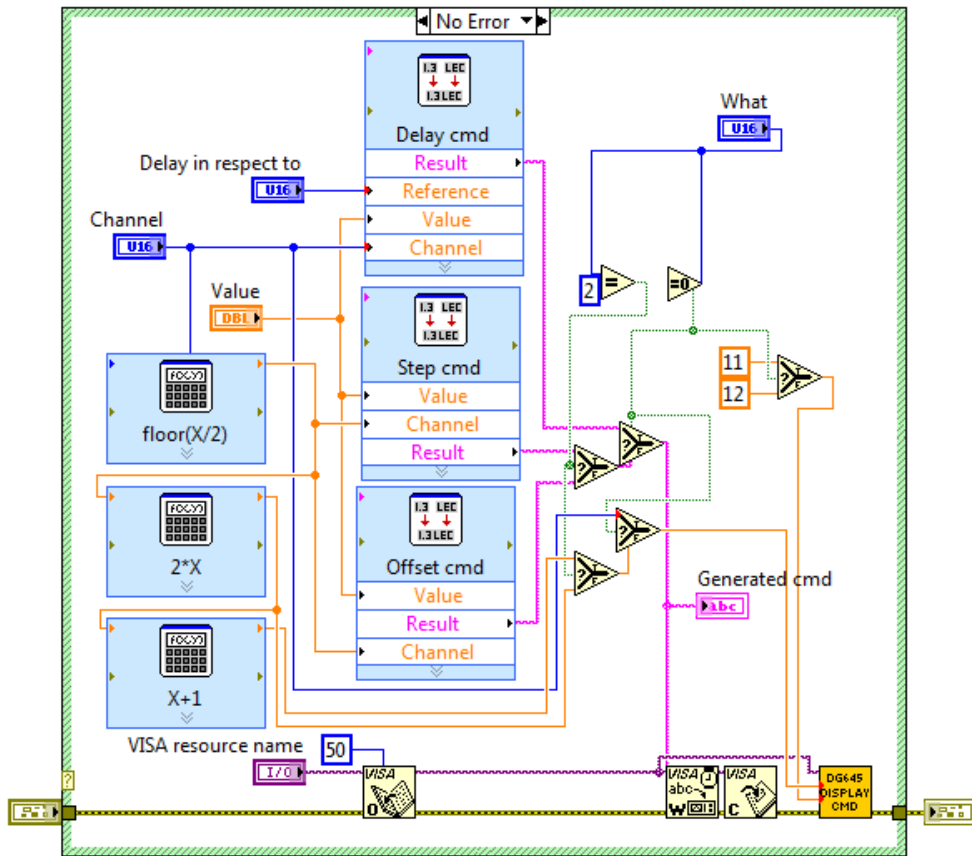


Figure 19: Another part of the driver.

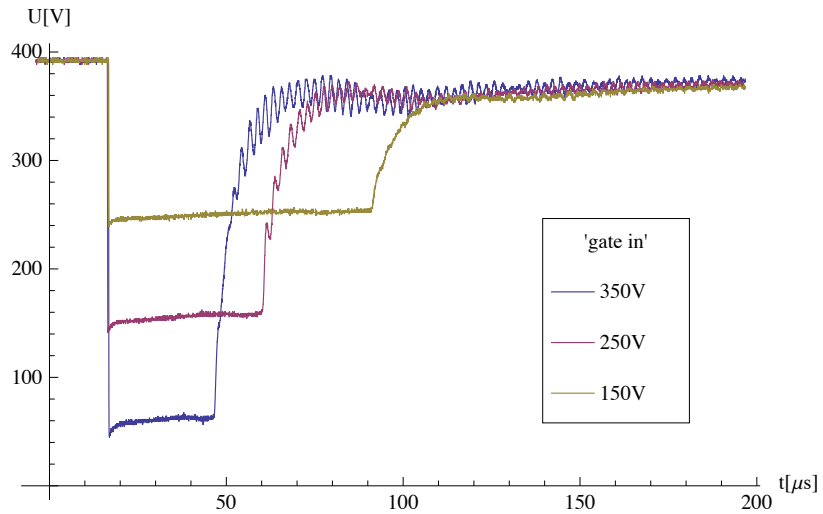


Figure 20:  $V_{fo}$  vs. time, with changing 'GATE' values.

## A.2 SE Measurements

Figure 20 to 22 show the measurement results without the optimization part. The oscillations in the voltage as well as the dependency on the 'IC SUPPLY' voltage are unwanted. Figure 23 to 25 show measurements after installing the optimization. The voltage oscillations are on an acceptable level now, but the timescale is stretched by a factor of  $\approx 10$ . The measurements after changing the polarization of 'TRIGGER' are shown in figure 25 and 27. The measurements shows all desired properties. A further description of Figure 20 to 27 can be found in Section 4.5 to 4.7.



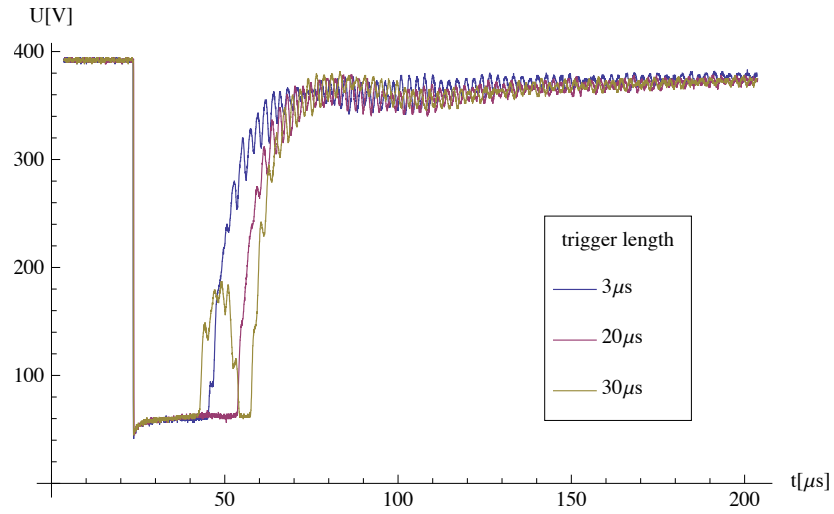


Figure 21:  $V_{fo}$  vs. time, with changing trigger-length, i.e. changing the time where 'TRIGGER' is set HIGH.

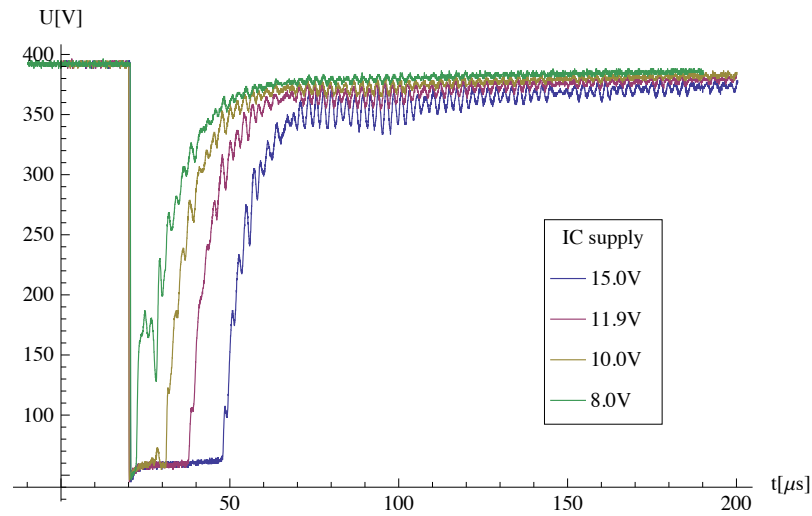


Figure 22:  $V_{fo}$  vs. time, with changing 'IC SUPPLY' voltage.

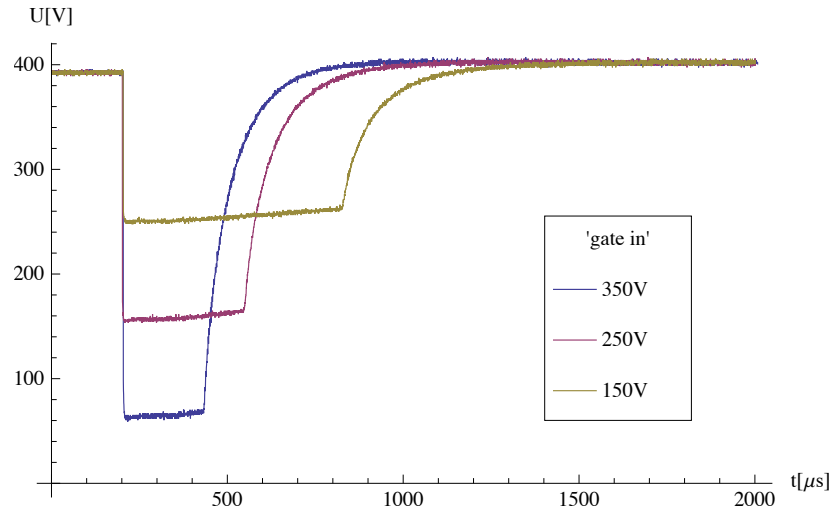


Figure 23:  $V_{fo}$  vs. time, with changing 'GATE' values after the Optimization.

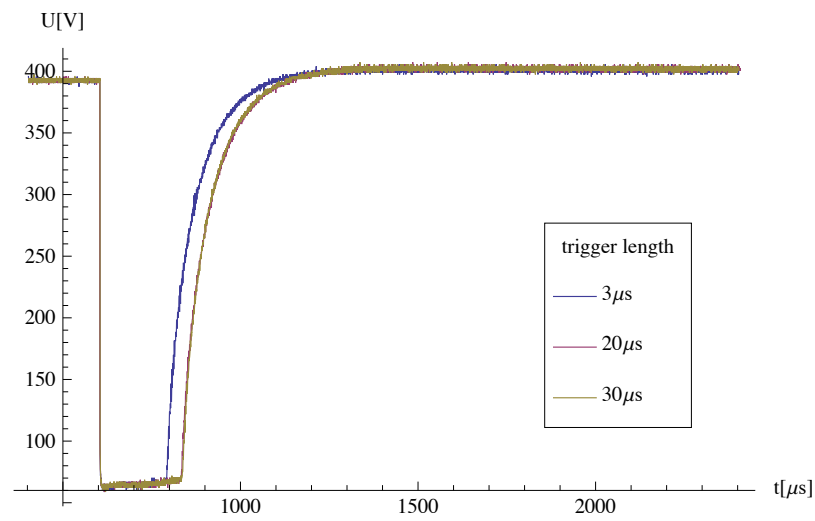


Figure 24:  $V_{fo}$  vs. time, with changing trigger-length, i.e. changing the time where the 'TRIGGER' is set HIGH.

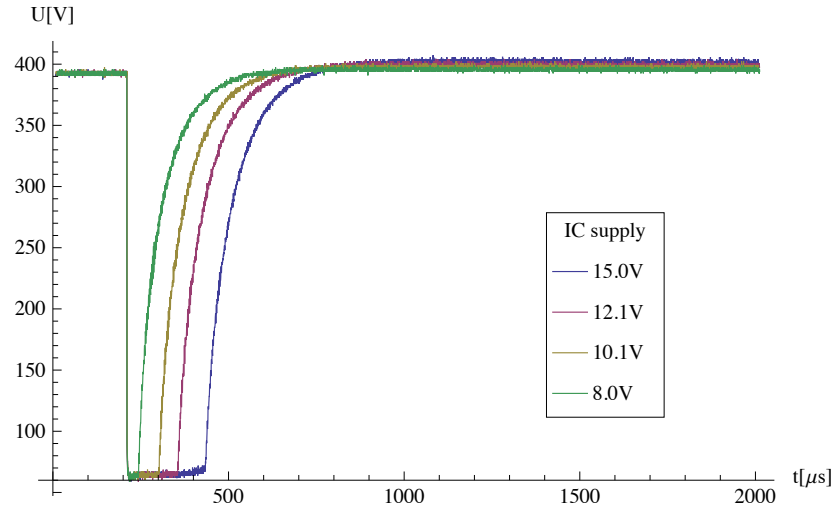


Figure 25: The IC supply voltage still has a big influence on the trigger-time.

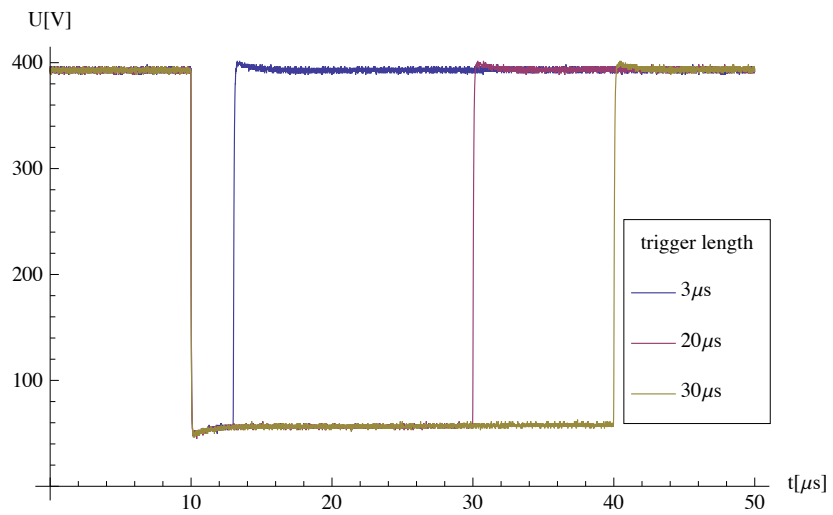


Figure 26:  $V_{fo}$  vs. time, with changing trigger-length, i.e. changing the time where the 'TRIGGER' is set HIGH.

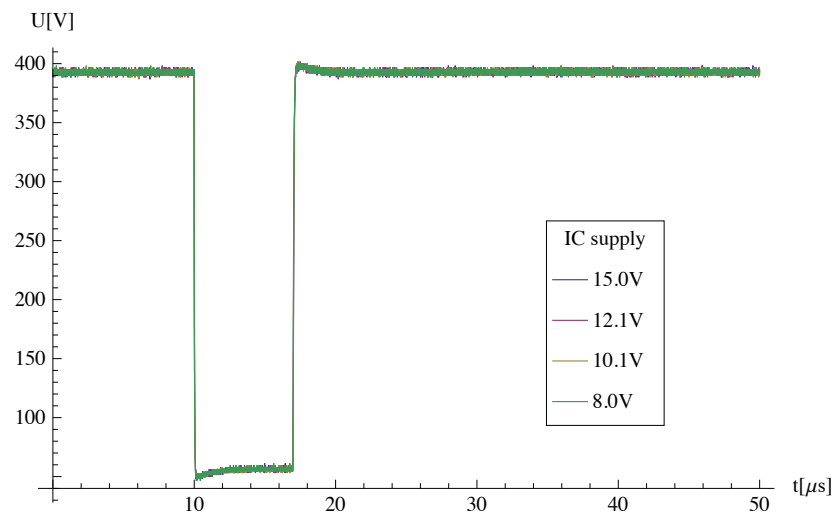


Figure 27: No dependence on the 'IC SUPPLY' in the range from 8 V to 15 V could be observed. Note that there are four graphs displayed in this plot on top of each other.

### A.3 Startup Procedure

This manual describes the startup procedure for the experimental setup. It was accurate up to June 2012 and may be outdated now since the experiment moved in another laboratory.

#### A.3.1 Start up procedure of the experiment setting

1. Turn on the valve voltage source. It's the lowest box in rack.
2. Open the helium gas bottle. Do this by opening the main valve fully and the secondary valve by a half turn.
3. Connect the filament power plug to the grid. Its located on the main experiment table. Slowly increase the voltage by turning the potentiometer until you reach 5.25 V (match indicator to the black line).
4. Turn on the HV that accelerates the electrons emitted by the filament toward the valve. It's the upper "Heinzinger" box of the three. You need to push two buttons (power on and voltage out).
5. Turn on the integrator power. Its located under the main experiment table.
6. Turn on the dye-pump. Its near to the laser-table.
7. Go to the laser panel (small laptop on the rack). If the Spitlight-programm runs already proceed with 10.
8. Start Spitlight GUI and choose connect from the connection menu.
9. Log in as privileged user in the login menu. The password is "Innolas".
10. Go to the trigger setting and change it to intern, apply and confirm.
11. Switch on the flash lamps with the key. Its at the same place as the dye-pump power.
12. Choose "start laser" and then "start pump" source.
13. Go again to the trigger setting and change it to extern, apply and confirm.
14. Wait for 20 minutes.
15. Press "open shutter" and wait for 15 minutes.
16. Open starlab at the log computer (129.132.60.252:16000). Select Vega... and press together.
17. Power measurement of the Nd:Yag laser: Insert the Vega sensor into the beam path of the Nd:Yag laser on the laser table. In starlab set Range to 400 mJ, wavelength to 532 nm and start logging. After 5 minutes note the average and the standard deviation in the lab journal.

18. Power measurement of the BlueDye laser: Insert the Vega sensor into the beam path of the BlueDye laser on the laser table. In starlab set Range to 4mJ, wavelength to 313 nm and start logging. After 5 minutes note the average and the standard deviation in the lab journal.
19. Copy the two log files from documents/starlab to M/log/LaserPowStability/LogStabLaser and change the names accordingly.
20. Remove laser blocker in order to get the laser in the experiment.
21. Turn on the MCP HV 'IC SUPPLY'. It's near the laser panel.
22. Switch on the Extraction HV. Turn it up slowly. (be sure that the HV-Switch is on).
23. Switch on the MCP (front/back) HV and the phosphor HV. If measuring electrons turn them on up simultaneous in order not to have too big potential differences.
24. Turn on the 'GATE'. Its behind the the HV boxes.
25. Have fun

### A.3.2 Changing polarity of the experiment

In order to switch from measuring positive ions to measuring electrons various things need to be changed. Described is the process from ions to electron (and vice versa in brackets). The exact potentials can be found in table 1:

1. Switch off all HV sources (phosphor, MCP back, MCP front, extraction) and the 'GATE'.
2. Switch off the HV-Switch.
3. Turn the switch of the HV-Switch to negative (positive).
4. Change the input HV cable at the bottom of the HV-Switch. The extraction HV-cable has to be connected with the negative input. The positive input need to be grounded with the cap. (the other way around).
5. At the MCP-HV-Switch remove MCP front-cable (MCP back-cable). Remove the the short HV-short from the MCP back ('MCP FRONT') and connect it with MCP front ('MCP BACK'). Then connect the MCP front-cable with the MCP front (back instead of front).
6. Switch the 'GATE' back on.
7. Slowly turn up the extraction, MCP back (MCP front) and the phosphor HV.
8. If one changes from ramped ionization to a square pulse ionization change also the corresponding trigger time.

HV Source	Positive Ion Mode	Electron Mode
Extraction	1.2 kV	-1.2 kV
MCP front	-2.4 kV	GND
MCP back	GND	2 kV
Phosphor	0.4 kV	2.8 kV
Gate	-0.35 kV	-0.35 kV

Table 1: These are the potentials needed to detect positive or negative particles.

## A.4 PCB Manufacture with the Etching Method

This is a short manual how to create self-made PCBs based on my experience. The process is similar to developing photographic pictures. The three steps are: exposition, development and fixation. The PCB from the PHYS-Shop has a photo-resist on top of copper-layer that is acid-proofed. This resist is damaged by UV-light and washed away in the development process. Therefore the exposed parts of the copper can be etched off, since the resist is removed. For the development and fixation process wear gloves and glasses.

### A.4.1 Preparations

You need to print a foil where the copper-parts that are supposed to remain on the PCB are printed in black. Where the foil is transparent, the copper will be etched off by the acid. Make them as black as possible since this consumes less acid afterward. All larger areas that do not have a circuit on it should therefore be black. Normal printer-foils printed with a laser-printer work great. Handle the printed foil with care, since every scratch in the colored surface may result in a broken connection. For ink-printer I recommend to set the quality to high, since the amount of ink is typically larger at high settings. PCBs for custom prints can be retrieved at the PHYS shop. Do not take off the protective foil on the PCB until you are in the etching lab.

### A.4.2 Exposition to UV-light

In the lab pay attention that you work only with the yellow light and closed door until the PCB is done, otherwise the UV-light of normal lights will destroy the photo-resist and the entire copper-layer will be etched off. Cut your PCB part a little bigger as you need it since the part that is in the holder of the acid bath is not etched properly. This part can be removed in the end. It's also recommended to switch on the UV-exposition-light for about 2 minutes before using it in order to heat up. Make sure that the lower light is switched on (both for double sided). After this step place your foil on the glass (think hard which way you put it!). Remove the protective foil (for double sided: don't throw it away, you'll need it later) from the PCB and place it face down onto your foil. Don't do it the other way, since the space between the glass and the cap will be evacuated. If you put a foil that is larger as the PCB on top of it, it may happen

because of the vacuum, the foil is bend a little and is not anymore flush with the PCB. This results in a bad exposition and thus the PCB will be defective. Let it exposed about 1.5 minutes. Prepare in the meantime the developer. For double sided PCB see A.4.6.

#### **A.4.3 Development**

Pour developer in a glass and insert your exposed PCB. Wait for two minutes and take it out. Wash it with water and proceed to the etching step. For double sided PCB: don't shake the glass while the PCB is in, because the bottom side can be damaged in process. I recommend to place the exposed PCB onto two thin PCB stripes so that the bottom side can also be fully developed. The stripes shouldn't touch parts of the bottom side that have circuits on it.

#### **A.4.4 Fixation with acid**

Take the washed developed PCB and mount it in the holder of the acid bath. Note that the part that is in the holder will not be etched off properly. Be quick since the acid bath smells very strong. Check after about 5 minutes if all the wanted copper-parts are etched of. If not, check after about every minute again. The time depends on the freshness<sup>7</sup> of the acid bath. But after 12 minutes it should be done. Take it out and wash it with water.

#### **A.4.5 Post-processing**

If you want to cut and/or drill the PCB do this now. For double layer: Put the protective foil back on the bottom side to avoid scratches in the process. As last step you need to remove the remaining photo-resist from the PCB, otherwise you won't be able to solder on it. This can be done with acetone. Dispose the acetone properly (not in the sink). Furthermore solder lacquer can be applied. It will protect the copper and helps preventing lead to connect with the copper in unwanted places.

#### **A.4.6 Double sided PCB**

In order to avoid the foil problem described in A.4.2. cut the top and the bottom foil a bit smaller than the PCB. Put the top foil on it and drill two holes on opposite edges at places that you can also recognize on the bottom foil. Remove the protective foil on both sides and mount the foils at the right places with tape. Proceed with A.4.2.

---

<sup>7</sup>pH of the acid



## List of Figures

1	picture from the qudev group . . . . .	2
2	picture from Tobias Thiele . . . . .	4
3	picture taken by Tobias Thiele . . . . .	6
4	modified version of the picture in the wikipedia article: <a href="http://de.wikipedia.org/wiki/Mikrokanalplatte">http://de.wikipedia.org/wiki/Mikrokanalplatte</a> (09.2013) . . . . .	6
5	picture from <a href="http://cdn.rohde-schwarz.com/product/dg645/DG645_front.jpg">http://cdn.rohde-schwarz.com/product/dg645/DG645_front.jpg</a> (09.2013) . . . . .	7
6	picture was taken from [7, p 46] . . . . .	8
7	picture from LabView program . . . . .	9
8	picture from LabView program . . . . .	10
9	created with LibreOffice Version 4.0.4 . . . . .	11
10	created with gEDA Schematic Editor 1.6.2 . . . . .	12
11	pictures taken by the author . . . . .	17
12	plotted with Wolfram Mathematica 8 for Students . . . . .	18
13	plotted with Wolfram Mathematica 8 for Students . . . . .	19
14	pictures taken by the author . . . . .	20
15	created with gEDA Schematic Editor 1.6.2 . . . . .	21
16	designed with OpenDraw 3.2.0 . . . . .	23
17	plotted with Wolfram Mathematica 8 for Students . . . . .	25
18	picture from LabView program . . . . .	27
19	picture from LabView program . . . . .	28
20	plotted with Wolfram Mathematica 8 for Students . . . . .	29
21	plotted with Wolfram Mathematica 8 for Students . . . . .	30
22	plotted with Wolfram Mathematica 8 for Students . . . . .	30
23	plotted with Wolfram Mathematica 8 for Students . . . . .	31
24	plotted with Wolfram Mathematica 8 for Students . . . . .	31
25	plotted with Wolfram Mathematica 8 for Students . . . . .	32
26	plotted with Wolfram Mathematica 8 for Students . . . . .	32
27	plotted with Wolfram Mathematica 8 for Students . . . . .	33

## References

- [1] Burr-Brown. <http://www.ti.com/lit/ds/symlink/opa627.pdf>.
- [2] Fairchild. <https://www.fairchildsemi.com/ds/fq/fqp5n60c.pdf>.
- [3] T.F. Gallagher. *Rydberg Atoms*. Cambridge Monographs on Atomic, Molecular and Chemical Physics. Cambridge University Press, 2005.
- [4] S. D. Hogan, P. Allmendinger, H. Saßmannshausen, H. Schmutz, and F. Merkt. Surface-electrode rydberg-stark decelerator. *Phys. Rev. Lett.*, 108(6):063008, Feb 2012.
- [5] intersil. <http://www.intersil.com/content/dam/intersil/documents/fn28/fn2853.pdf>.
- [6] Photonis. [http://www.sii.co.jp/jp/segg/files/2013/04/file\\_image\\_file\\_5260\\_image02.pdf](http://www.sii.co.jp/jp/segg/files/2013/04/file_image_file_5260_image02.pdf).
- [7] SRS. <http://www.thinksrs.com/downloads/pdfs/manuals/dg645m.pdf>.
- [8] A. Wallraff. Quantenmechanik mit Schaltkreisen: Photonen und qubits auf einem supraleitenden Mikrochip. *Physik Journal*, 7(12):39–45, 2008.



Eidgenössische Technische Hochschule Zürich  
Swiss Federal Institute of Technology Zurich

## Declaration of originality

The signed declaration of originality is a component of every semester paper, Bachelor's thesis, Master's thesis and any other degree paper undertaken during the course of studies, including the respective electronic versions.

Lecturers may also require a declaration of originality for other written papers compiled for their courses.

I hereby confirm that I am the sole author of the written work here enclosed and that I have compiled it in my own words. Parts excepted are corrections of form and content by the supervisor.

**Title of work** (in block letters):

Design, Build-up and Control of Electronic Equipment for the Hybrid Rydberg Experiment

**Authored by** (in block letters):

*For papers written by groups the names of all authors are required.*

**Name(s):**

Koenz

**First name(s):**

Mario Silvester

With my signature I confirm that

- I have committed none of the forms of plagiarism described in the '[Citation etiquette](#)' information sheet.
- I have documented all methods, data and processes truthfully.
- I have not manipulated any data.
- I have mentioned all persons who were significant facilitators of the work.

I am aware that the work may be screened electronically for plagiarism.

**Place, date**

Zuerich, 12 Mai 2014

**Signature(s)**

*For papers written by groups the names of all authors are required. Their signatures collectively guarantee the entire content of the written paper.*